Multi-Fiber Blended Needle-Punched Nonwoven With Oleophilic and Self-Cleaning Properties for Oil Spill Cleanup

Article *in* Advanced Materials Technologies · January 2025

DOI: 10.1002/admt.202401628

5 authors, including:

Hanur Meku Yesuf
Bahir Dar University and Donghua University
19 PUBLICATIONS **152** CITATIONS
SEE PROFILE

Syed Rashedul Islam
Uttara University
66 PUBLICATIONS **477** CITATIONS
SEE PROFILE

Xueping Zhang
Donghua University
66 PUBLICATIONS **3,910** CITATIONS
SEE PROFILE

ADVANCED MATERIALS TECHNOLOGIES
www.advmattechnol.de

Multi-Fiber Blended Needle-Punched Nonwoven With Oleophilic and Self-Cleaning Properties for Oil Spill Cleanup

Hanur Meku Yesuf, Merem Hassen Aweke, Syed Rashedul Islam, Xueping Zhang, and Xiaohong Qin**

This study investigates the self-cleaning, oleophilic, and oil spill clean-up properties of multi-fiber blended needle-punc lf-cleaning performance of the nonwoven fabrics is influenced by the fiber composition. All samples with a low overall surface energy of 27.65–33.46 mN m^{-1}, especially those with a reduced polar component, demonstrate superior oil sorption of 13.83–19.45 g g^{-1} and retention capabilities of 91.11–98.83%. Oil-to-water selectivity of 13.66–42.60 and oil removal efficiency of 93.18–97.71% are achieved. The initial oil recovery rate (desorption) during the first desorption cycle (D1) ranges from 78.28% to 79.88%. This recovery rate remains consistently high, between 97.38% and 99.86%, throughout the second to tenth desorption cycles (D2 to D10) for all samples. The findings demonstrate that the blending of multi-fibers and web arrangement play a critical role in enhancing oil sorption and retention, oil selectivity, oil removal efficiency, reusability and self-cleaning with statistically significant performance ($p < 0.05$).

1. Introduction

Oil spills cause lasting ecological damage, threatening biodiversity and habitat integrity.[1–6] Prompt and effective cleanup of oil spills is essential to mitigating their severe environmental, economic, and public health impacts.[2,5,6] Sorption materials are commonly used to remove the oil spilled from water by mechanically extracting oil from water. Nonwoven fabrics, particularly needle-punched nonwoven fabrics, have proven effective in oil spill remediation due to their unique structure and properties.[7–15]

Previous studies have demonstrated the effectiveness of needle-punched nonwoven fabrics in oil spill remediation. For example, nonwoven fabrics made from recycled polyester fibers,[3] natural and synthetic blends like nettle and polypropylene,[4] and kapok/polypropylene[16] blends have shown high oil sorption capacities, making them suitable for oil spill contaminant absorption. Polymeric sorbents, with their higher surface area and loading capacity, offer superior oil absorption, rapid kinetics, and easy recovery, along with enhanced pH stability for use in extreme separation conditions compared to traditional sorbents.[17]

Other researchers have explored the potential of biodegradable porous fibrous membranes, such as polylactic acid (PLA) fibrous membrane,[18] polyacrylonitrile-based nanocomposite,[19] PLA/PEO,[20] and degummed silk modified with electrospun polylactic acid (DG-Silk/PLA),[21] for oil-water separation and oil absorption. Additionally, polyacrylonitrile (PAN)[22] and polyphenylene sulfide (PPS)[23,24] fibers have been developed into superhydrophobic nonwovens and fibrous membranes, exhibiting impressive performance in oil-water separation and industrial applications. These materials not only offer efficient oil sorption but also demonstrate excellent reusability, maintaining significant adsorption capacities after multiple cycles.[21]

In this study, fibers such as polylactic acid (PLA), polyphenylene sulfide (PPS), polyacrylonitrile (PAN), polypropylene (PP), and polyester (PET) were selected for their unique properties and then blended in different proportions and web arrangement to create needle-punched nonwoven samples. PAN fibers are recognized for their exceptional strength and thermal stability, contributing to nonwoven fabrics' dimensional stability and

H. M. Yesuf, S. R. Islam, X. Zhang, X. Qin
Key Laboratory of Textile Science & Technology
Ministry of Education
College of Textiles
Donghua University
Shanghai 201620, China
E-mail: xpzhang@dhu.edu.cn; xhqin@dhu.edu.cn
H. M. Yesuf
Textile Engineering
Ethiopian Institute of Textile and Fashion Technology
Bair Dar University
P.O. Box, Bahir Dar 1037, Ethiopia
M. H. Aweke
M10-003
Bahir Dar University
Bahir Dar 6000, Ethiopia
S. R. Islam
Department of Textile Engineering
Uttara University
Dhaka 1230, Bangladesh
S. R. Islam
Department of Textile Engineering
Apparel Manufacture and Technology
BGMEA University of Fashion and Technology
Dhaka 1350, Bangladesh

The ORCID identification number(s) for the author(s) of this article can be found under https://doi.org/10.1002/admt.202401628

DOI: 10.1002/admt.202401628

durability.[12,13,25–28] They exhibit strong resistance to chemicals and abrasion, making them a reliable choice for various applications. PET fibers are commonly used in nonwoven materials due to their high tensile strength and remarkable resilience.[12,13,29–32] These fibers resist stretching and shrinkage effectively, offering durability while being resistant to moisture, mildew, and a wide range of chemicals.

PLA fibers are sourced from renewable materials, rendering them an environmentally friendly option.[12,13,33–36] They provide comfort, softness, and breathability, and are biodegradable, resulting in a lower carbon footprint compared to conventional synthetic fibers. PP fibers are lightweight yet possess high tensile strength, along with excellent resistance to moisture, chemicals, and abrasion.[12,13,37–40] They also provide good thermal insulation properties. PPS fibers are notable for their high chemical resistance and ability to withstand elevated temperatures.[12,13,28,41–43] They offer excellent dimensional stability and resistance to creep, as well as effective electrical insulation properties.

The aim of blending these fibers was to leverage the performance of each fiber to produce versatile, high-performing materials. The study specifically evaluated the self-cleaning, oil sorption and retention, and water-oil-selectivity and reusability properties of the fabrics. The findings of this research provide valuable insights into the potential of combining different fiber types and functional treatments for applications in oil spill cleanup. The results highlight the effectiveness of these innovative materials in addressing critical environmental challenges while demonstrating the benefits of using advanced fiber technologies.

2. Experimental Section

2.1. Materials

Eight needle-punched nonwoven samples with different fiber blend ratios were prepared at Donghua University, Shanghai, China. The study investigated various fiber blends and web arrangements in needle-punched nonwoven samples. N0, N1, and N2 all had an equal blend of 20% PAN, 20% PET, 20% PLA, 20% PP, and 20% PPS, but with different web arrangements: N0 used a cross-laid web, N1 had a parallel-laid web, and N2 had a pre-needled parallel-laid web. The remaining samples (N3–N7) utilized a parallel-laid web arrangement but varied the fiber blend, with each sample having one dominant fiber at 60% while the other four fibers were reduced to 10%. Specifically, N3 had 60% PAN, N4 had 60% PET, N5 had 60% PLA, N6 had 60% PP, and N7 had 60% PPS. The comprehensive details of sample preparation were presented in this previous publication.[12,13] For the oleophilic testing, two types of oils—Food oil and engine oil—were employed. Their densities and surface tensions were determined using a Tensionmeter (DCAT11, Dataphysics, Germany). Viscosities of the oils were measured by SNB2 Digital Rotary Viscosimeter. The surface tension, density, and viscosity of food oil were 33.12 mN m^{-1}, 0.87 g cm^{-3}, and 65.42 mPa.s respectively. Surface tension, density, and viscosity of engine oil were 27.79 mN m^{-1}, 0.81 g cm^{-3}, and 156.35 mPa.s respectively.

2.2. Characterization

2.2.1. Standard Test Methods

The test method and the experimental procedures were performed based on the standard test method. Before the test, all samples were conditioned under a standard atmosphere at a temperature of 20 ± 2 °C and a relative humidity of 65% for 24 h.

2.2.2. SEM Analysis

A Hitachi Flex-SEM (scanning electron microscopy) 1000 (SU1000) was used to examine the morphology of the needle-punched fabric fibers. To enhance image quality, all samples were sputter-coated with a thin layer of gold before analysis.

2.2.3. Self-Cleaning Test

In this test, to evaluate the self-cleaning ability of multi-fiber blended needle-punched nonwoven samples, coffee powder was chosen as the model pollutant, and polyester fabric was used for comparison. For the test, the coffee powder boiled with water was placed on the surface samples and then drained from the surface to remove the pollutant droplets. It was also checked by a continuous flow of the pollutant coffee liquid on the surface of the samples.

2.2.4. Water Contact Angle Test

An optical video contact angle instrument (Model KINO SL200KS) was used to determine the water contact angle of the fabric samples. A 10 ml water droplet was dispensed onto each sample, and the contact angle was measured over 180 seconds to capture any dynamic changes. The average contact angle for each sample was calculated based on measurements from five different areas. All testing was conducted at a controlled temperature of 20 ± 2 °C.

2.2.5. Oil Sorption and Retention Test

The ASTM F 716–09 standard was utilized to ascertain the oil absorption capacity.[44] For 15 minutes, the nonwoven sorbent (3 cm^2) was immersed in 150 mL of oil to trap the oil until there was no noticeable weight change. The needle-punched nonwoven sorbent was swapped out, laid on wire mesh, and allowed to drain to remove any leftover oil. The oil absorption and retention capacity were measured by averaging three and five repetitions. The test was conducted at a constant temperature of 22 ± 2 °C. The oil sorption and oil retention capacities were calculated using Equations (1) and (2) respectively.[45–47]

$$O_S = \frac{W_2 - W_1}{W_1} \times 100 \quad (1)$$

$$O_R = \frac{W_3 - W_1}{W_2 - W_1} \times 100 \quad (2)$$

Table 1. Surface energies of samples details.

Sample	Probe liquids	Surface tension of probe liquids [mN m^{-1}]			Contact angles [°]	Surface energies of samples [mN m^{-1}]		
		γ^d_L	γ^p_L	γ_L		γ^d_S	γ^p_S	γ_S
N0	Diiodomethane	50.8	0	50.80	57.95	29.76	1.86	31.62
	Water	19.90	52.20	72.10	126.77			
N1	Diiodomethane	50.8	0	50.80	57.28	30.14	1.87	32.01
	Water	19.90	52.20	72.10	126.47			
N2	Diiodomethane	50.8	0	50.80	58.48	29.45	1.78	31.23
	Water	19.90	52.20	72.10	126.56			
N3	Diiodomethane	50.8	0	50.80	54.63	31.66	1.10	32.75
	Water	19.90	52.20	72.10	120.90			
N4	Diiodomethane	50.8	0	50.80	*56.98*	30.31	1.63	31.94
	Water	19.90	52.20	72.10	125.07			
N5	Diiodomethane	50.8	0	50.80	52.71	32.75	0.71	33.46
	Water	19.90	52.20	72.10	117.42			
N6	Diiodomethane	50.8	0	50.80	65.67	25.32	2.33	27.65
	Water	19.90	52.20	72.10	133.12			
N7	Diiodomethane	50.8	0	50.80	64.06	26.24	2.36	28.61
	Water	19.90	52.20	72.10	132.40			

where O_S = oil sorption, O_R = oil retention, W_1 = the weight of the dried needle-punched nonwoven sorbent before sorption in gram, W_2 = the total weight of wetted needle-punched nonwoven sorbent after oil draining out for 15 min in gram, and W_3 = the weight of wetted needle-punched nonwoven sorbent after 24 h dripping in gram.

2.2.6. Surface Energy Test

Owens-Wendt-Rabel-Kaelble (OWRK) method, as described by Owens and Wendt in 1969, establishes a relationship between the surface energy of a liquid and the surface energy of a solid, as shown in Equation (3). This method was used to determine the surface energies of the needle-punched nonwoven samples. Equation (3) was expressed in terms of Equations (4) and (5) to calculate the polar component of sample surface energy by using two different liquids, namely water and methylene iodide (Diiodomethane (CH_2I_2)) respectively. Then by using simultaneously Equations (4–6) was derived to calculate the dispersion component of sample surface energy. Finally, the sample surface energy was determined by summation of the polar and dispersion components of sample surface energy, Equation (7). The surface tensions of liquids and the corresponding contact angles were given in **Table 1**.

$$\frac{\gamma_l(1+\cos\theta)}{2} = \left(\sqrt{\gamma_s^d\gamma_l^d} + \sqrt{\gamma_s^p\gamma_l^p}\right) \tag{3}$$

$$\frac{\left(\left(\frac{\gamma_{lw}(1+\cos\theta_w)}{2}\right) - \sqrt{\gamma_s^d\gamma_{lw}^d}\right)^2}{\gamma_{lw}^p} = \gamma_s^p \tag{4}$$

$$\frac{\left(\left(\frac{\gamma_{ll}(1+\cos\theta_l)}{2}\right) - \sqrt{\gamma_s^d\gamma_{ll}^d}\right)^2}{\gamma_{ll}^p} = \gamma_s^p \tag{5}$$

$$\frac{\gamma_{ll}^p\gamma_{lw}^2(1+\cos\theta_w)^2 - \gamma_{lw}^p\gamma_{ll}^2(1+\cos\theta_l)^2}{4\left(\gamma_{lw}^d\gamma_{ll}^p - \gamma_{ll}^d\gamma_{lw}^p\right)} = \gamma_s^d \tag{6}$$

$$\gamma_s = \gamma_s^d + \gamma_s^p \tag{7}$$

where:

γ_l, liquids surface energy
θ, contact angle for liquids
γ_s^d, dispersion component of solid surface energy
γ_l^d, dispersion component of liquid surface energy
γ_s^p, polar component of solid surface energy
γ_l^p, polar component of liquid surface energy
γ_{lw}, liquid water surface energy
θ_w, contact angle for liquid water
γ_{lw}^d, dispersion component of liquid water surface energy
γ_{lw}^p, polar component of liquid water surface energy
γ_{ll}, liquid CH_2I_2 surface energy
θ_l, contact angle for liquid CH_2I_2
γ_{ll}^d, dispersion component of liquid CH_2I_2 surface energy
γ_{ll}^p, polar component of liquid CH_2I_2 surface energy

Statistical Analysis

One-way ANOVA was employed to identify significant differences in oil sorption and retention properties between samples (Table 5). The validity of the statistical methods relies on the assumptions of normality and homogeneity of variances. Normality was assessed visually using histograms, and Levene's test was

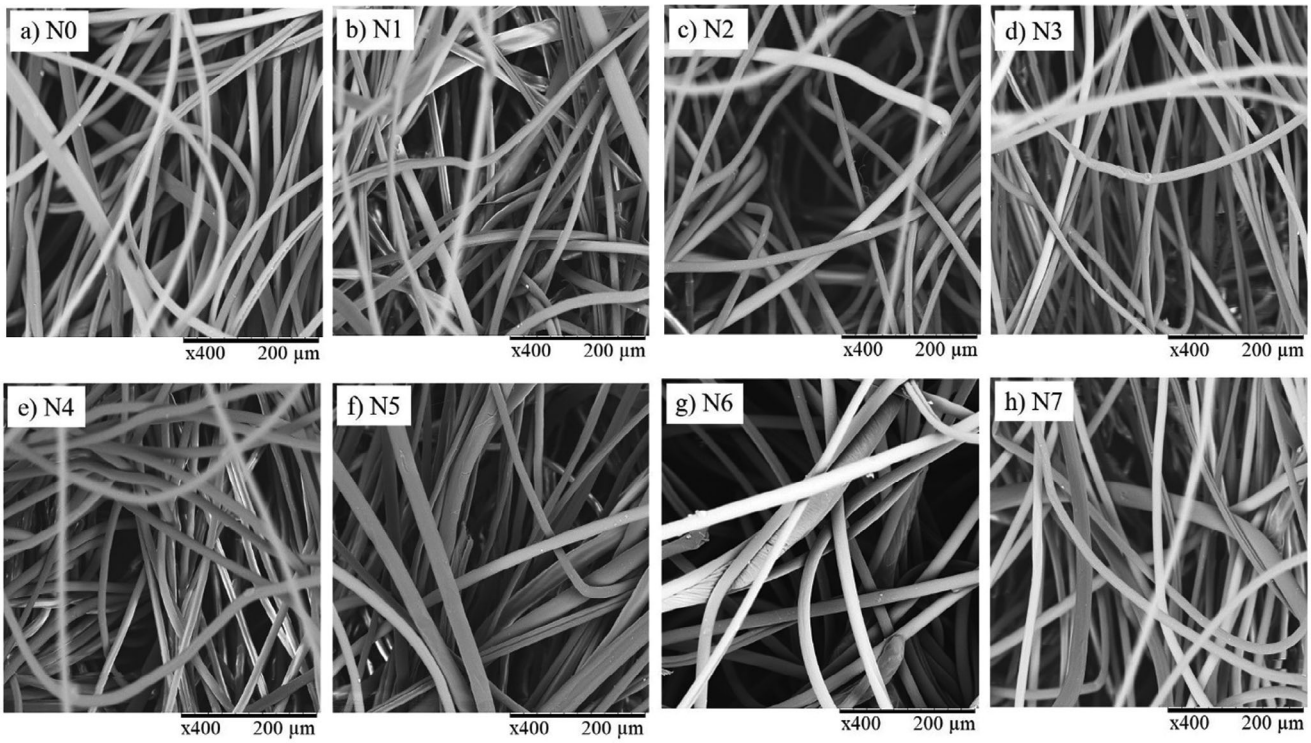

Figure 1. SEM images of needle-punched samples' surface views.

used to verify the homogeneity of variances. As both assumptions were met, the application of ANOVA was deemed appropriate.

3. Results and Discussion

3.1. Morphology of Samples

Figure 1 presents SEM images that illustrate the microstructure of various needle-punched nonwoven samples (N0 to N7), highlighting differences in fiber arrangement based on composition, fabric density, and porosity. Sample N0, with equal fiber proportions and a cross-laid web arrangement, has the highest fabric density (121.34 Kg m^{-3}) and lowest porosity (89.96%), reflected in its compact fiber structure. In contrast, N1, which shares the same fiber composition but features a parallel-laid arrangement, shows reduced density (90.96 Kg m^{-3}) and increased porosity (92.47%), resulting in a more open structure. Sample N2, with a pre-needled parallel-laid web, further reduces density (83.40 Kg m^{-3}) and increases porosity (93.11%), displaying an even looser fiber network.

Samples N3 to N7 vary in fiber composition, affecting their microstructure. N3, with 60% PAN and a parallel-laid arrangement, has a higher density (112.44 Kg m^{-3}) and porosity (90.75%), showing a more uniform structure. N4, dominated by 60% PET, exhibits moderate density (106.27 Kg m^{-3}) and porosity (91.26%), while N5, with 60% PLA, has the lowest density (81.70 Kg m^{-3}) and highest porosity (93.28%), showing a more open network. N6, composed of 60% PP, presents lower density (86.42 Kg m^{-3}) and high porosity (92.89%), with a dispersed fiber arrangement. N7, containing 60% PPS, shows higher density (109.36 Kg m^{-3}) and porosity (91.01%), reflecting a denser and more uniform fiber structure. The SEM images demonstrate that higher fabric density corresponds to more compact structures (e.g., N0, N3, N7), while higher porosity leads to more open arrangements (e.g., N2, N5), highlighting the impact of fiber composition on the material properties of nonwovens.[12,13]

3.2. Self-Cleaning

Before the coffee liquid was dropped on the samples (**Figure 2a**), all samples appeared uniformly clean, with no visible marks or stains. This baseline condition indicates that the fabric surfaces are initially uncontaminated, allowing for a clear assessment of the self-cleaning ability after exposure to coffee. During the coffee liquid drop on the samples (Figure 2b), the interaction between the liquid and the fabric provided insights into the hydrophobic properties of each blend. All samples except the control fabric showed the coffee forming a nearly spherical droplet, indicating better liquid repellence.

After removing the coffee droplet (Figure 2c), the samples exhibited varying degrees of staining. The control sample fabric showed a clear stain, indicating poor self-cleaning and high absorbency. N3, N6, and N7 appear to have the least staining, suggesting better self-cleaning performance, due to the higher content of PAN, PP, and PPS, which are known for their hydrophobic properties. Similarly, N0, N1, and N2 showed better self-cleaning performance, due to the equal content of fibers and varying web arrangement. N4 and N5 show more prominent staining, indicating that these blends are less effective at repelling the coffee

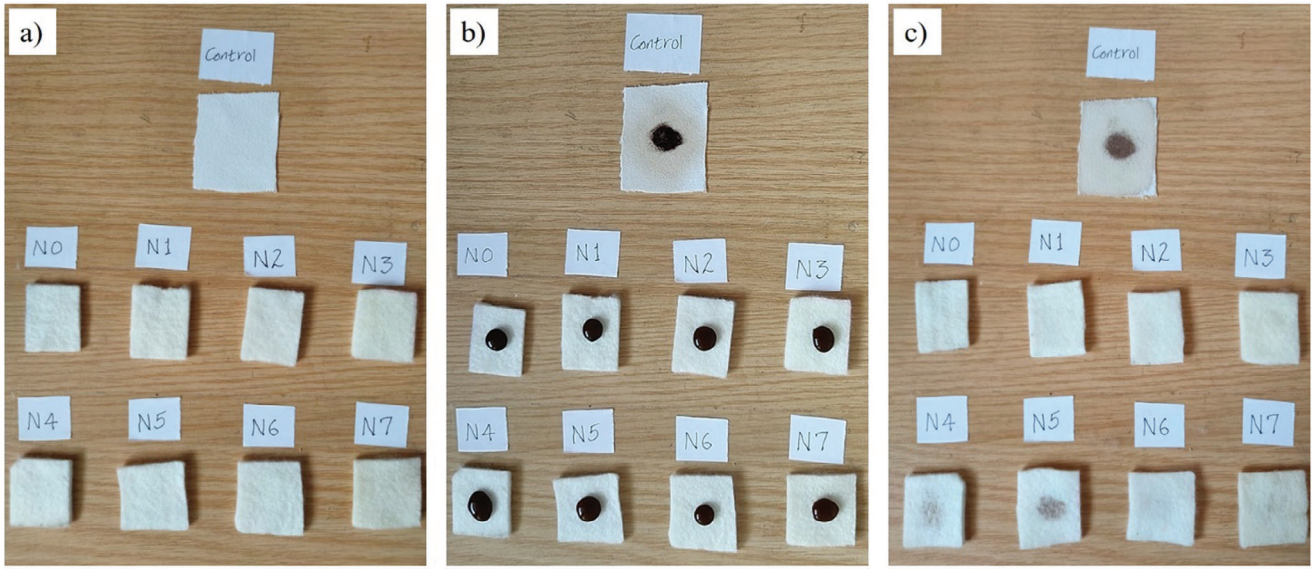

Figure 2. a) before the coffee liquid dropped on the samples, b) during the coffee liquid drop on the samples, c) after the coffee liquid droplet was removed from the samples.

liquid, potentially due to the higher PET and PLA content, which are known for their moderate hydrophobic properties.

3.3. Surface Energy

Table 1 provides data on the surface energies of different samples measured using probe liquids (diiodomethane and water). The surface energies of all samples (range from 27.65 to 33.46 mN m^{-1}) are far below the surface tension of water (72.8 mN m^{-1}), which indicates that all surfaces are likely to repel water molecules. The surface energy analysis concerning oil sorption and retention shows that samples with a balanced combination of high dispersive and appropriate polar components tend to have higher oil retention and good initial sorption capacities. Samples N6 and N7 demonstrate the best overall performance due to their optimized surface energies of 27.65 and 28.61 mN m^{-1} respectively, supporting effective oil sorption and retention as shown in **Table 2**.

The effectiveness of a material as an oil absorbent is closely linked to its surface properties. Materials with low surface energy, particularly those with a dominant dispersive component, excel at absorbing oil while repelling water.[48] This is because they have a stronger affinity for non-polar substances like oil compared to water. In essence, hydrophobic materials (water-repellent) and oleophilic (oil-attracting) make the best oil absorbents.[49] Our findings indicate that samples with lower overall surface energy, especially those with a reduced polar component, demonstrate superior oil sorption and retention capabilities.

3.4. Oil Sorption and Retention

Figure 3 demonstrates the process of oil sorption and retention in a sample material. The sequence included dipping the sample into oil, allowing excess oil to drip off, and then applying pressure to squeeze out additional oil. The mass of the sample was measured at various stages to assess its oil absorption and retention capacity. Table 2 presents a comparative analysis of various samples in terms of their ability to absorb and retain both food and engine oil. The data suggests that the samples exhibit varying degrees of oil sorption and retention capacities, which are

Table 2. Comparative analysis of food and engine oil sorption/retention of samples details.

Samples	N0	N1	N2	N3	N4	N5	N6	N7
Food oil sorption (g g^{-1})	14.58	16.87	18.29	17.15	17.60	15.83	19.45	18.78
Engine oil sorption (g g^{-1})	13.83	15.58	16.82	15.97	16.41	14.54	18.26	17.59
Food oil retention (%)	94.46	92.12	92.87	94.38	93.19	91.11	95.33	97.93
Engine oil retention (%)	96.04	93.55	94.18	95.70	94.51	92.38	97.02	98.83
Water sorption (g g^{-1})	0.49	0.73	0.57	0.63	1.07	1.06	0.46	0.66
Food oil-to-water selectivity	29.77	23.02	31.87	27.19	16.42	14.88	42.60	28.27
Engine oil-to-water selectivity	28.24	21.26	29.32	25.31	15.31	13.66	40.00	26.49
Food oil removal efficiency (%)	96.75	95.84	96.96	96.45	94.26	93.70	97.71	96.58
Engine oil removal efficiency (%)	96.58	95.51	96.70	96.20	93.87	93.18	97.56	96.36

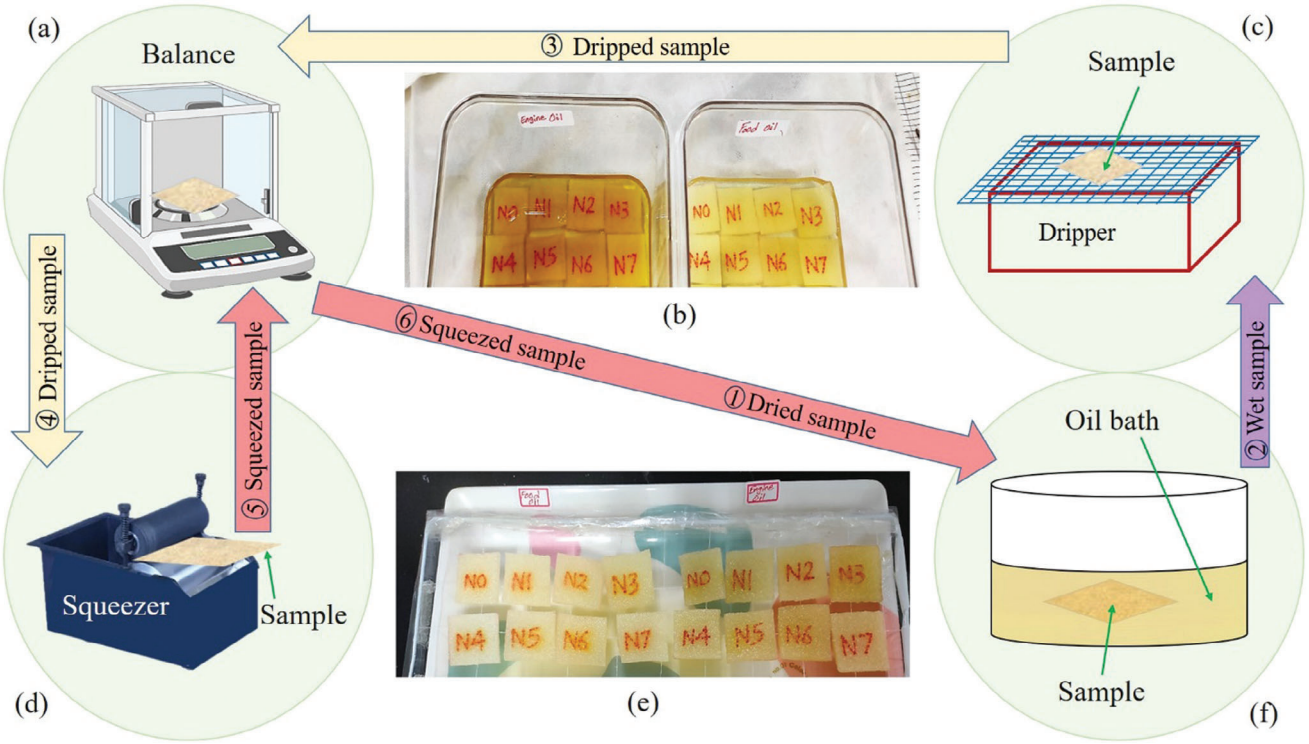

Figure 3. Oil Sorption/retention mechanism; a) weight balance, b) Samples dip into engine and food oil, c) drippings, d) squeezing mechanism, e) samples dripping, f) dipping mechanism.

influenced by factors such as fiber type, web arrangement, and blending ratios. The samples have been ranked from highest to lowest oil sorption capacity as N6, N7, N2, N4, N3, N1, N5, and N0. The highest food and engine oil sorption is observed in sample N6 with 19.45 g g^{-1} and 18.26 g g^{-1}, respectively. Sample N6, a blend of 60% PP and 10% of other fibers with a parallel-laid web arrangement, consistently outperforms others in both food and engine oil sorption. Higher percentages of PP and the cumulative effect of other fibers contribute positively to the oil sorption due to their highly hydrophobic and oil affinity properties. Parallel-laid web arrangements, low fabric density, and high porosity of sample N6[12,13] also have an impact on higher oil sorption as they provide more open, uniform, and aligned fiber structures, enhancing capillary action.

The lowest food and engine oil sorption is observed in sample N0 with 14.58 g g^{-1} and 13.83 g g^{-1}, respectively. Sample N0, with a cross-laid arrangement and equal fiber blending, shows the lowest sorption capacities in both food and engine oil. Equal percentages of fibers contribute to optimum oil sorption. However, cross-laid web arrangements, higher fabric density, and low porosity of sample N0[12,13] have a negative impact on oil sorption as they provide tighter fiber structures and more tortoise path, reducing capillary action.

Depending on fiber type, web arrangement, and blending ratios, the samples have been ranked from highest to lowest oil retention capacity as N7, N6, N0, N3, N4, N2, N1, and N5. Sample N7, a blend of 60% PPS and 10% of other fibers with a parallel-laid web arrangement, consistently outperforms others in both food and engine oil retention. This sample demonstrated exceptional retention for both food and engine oil, with rates of 97.93% and 98.83%, respectively. Higher percentages of PPS and the cumulative effect of other fibers contribute positively to oil retention due to their highly hydrophobic and oil affinity properties. Less porosity and high fabric density of sample N7[12,13] also resulted in its ability to trap oil effectively as they provide tighter fiber structures and more tortoise path, reducing capillary action.

The lowest food and engine oil retention is observed in sample N5 with 91.11% and 92.38%, respectively. Sample N5, a blend of 60% PLA and 10% of other fibers with a parallel-laid web arrangement, shows the lowest retention capacities in both food and engine oil. Higher percentages of PLA and the cumulative effect of other fibers contribute negatively to oil retention due to their less hydrophobic and oil affinity properties. High porosity and less fabric density of sample N5[12,13] also have an impact on lower oil retention as they provide loose and open fiber structures, increasing capillary action. Sample N3 and N4 have moderate sorption and retention due to their moderate hydrophobic, fabric density, and porosity properties. Sample N2 shows good food and engine oil sorption but has lower oil retention due to its pre-needling effect. Both the type of fibers used, blending ratio and their arrangement in the web play critical roles in determining the oil sorption and retention efficiency. All samples exhibit the best overall performance of food and engine oil sorption and retention, making them potentially suitable for applications demanding high oil sorption and retention.

Thilagavathi G, et al., have developed a kapok/polypropylene (80/20) needle-punched nonwoven fabric for oil spill cleanup,

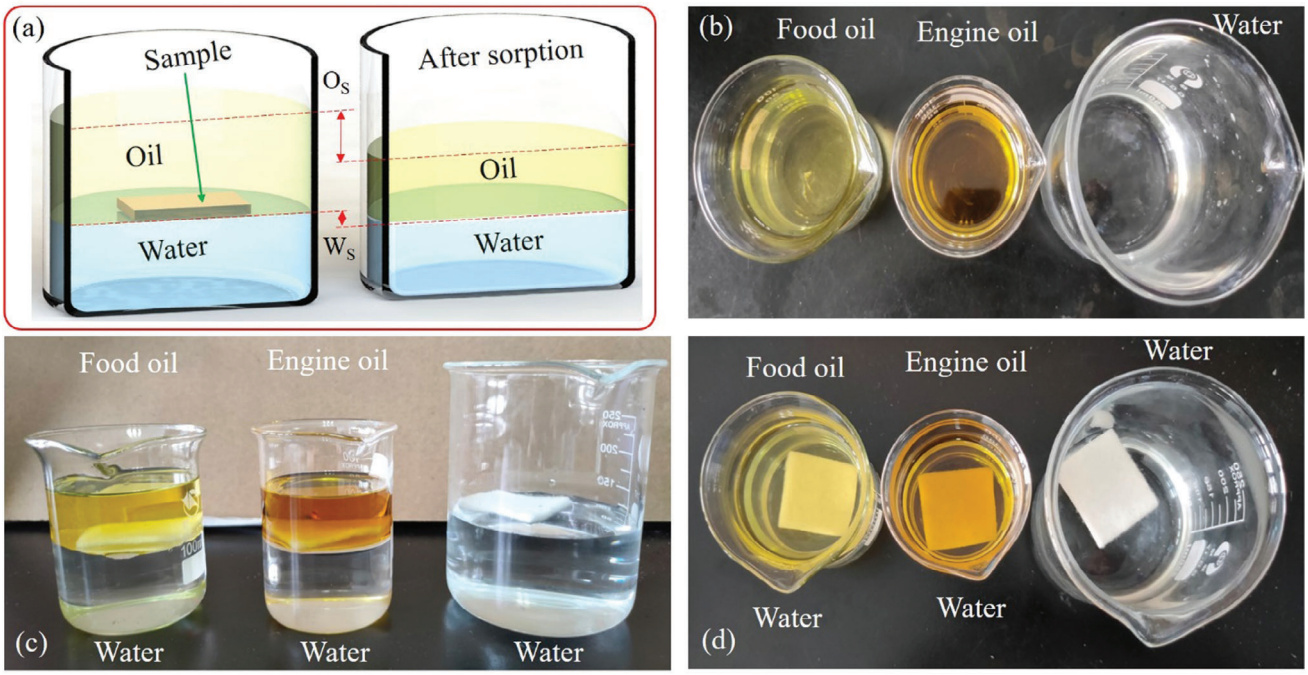

Figure 4. a) Oil-to-water selectivity testing mechanism; b) Food oil, engine oil and water; c) Oil-to-water selectivity testing side view; d) Oil-to-water selectivity testing top view.

achieving maximum oil sorption of 40.80 g g^{-1} and 29.0 g g^{-1} for high density oil (HD) and diesel oil respectively with retention values ranging from 0.88 to 1.00.[16] Zhang T, et al., prepared a polylactic acid (PLA) fibrous membrane with an oil-saturated adsorption capacity ranging from 32.28 g g^{-1} to 19.50 g g^{-1}, significantly outperforming the commercial nonwoven polypropylene, which had a capacity of only 9.34 to 7.79 g g^{-1}.[18] Momenzadeh Z, et al., demonstrated that highly efficient polyacrylonitrile-based nanocomposite sorbents, with an initial adsorption capacity of 12.47 g g^{-1}, showed excellent reusability, maintaining a capacity of about 10 g g^{-1} after five cycles in the oil spill removal process.[19] Compared to previous studies, the samples in this study, with lower overall surface energy (27.65–33.46 mN m^{-1}) and a reduced polar component, exhibited significantly improved oil sorption, ranging from 13.83 to 19.45 g g^{-1}, and retention capabilities of 91.11% to 98.83%. Additionally, these samples achieved oil-to-water selectivity between 13.66 and 42.60, along with oil removal efficiencies of 93.18% to 97.71%.

3.5. Oil-To-Water Selectivity

Oil-to-water selectivity refers to the ability of a material to preferentially absorb oil while minimizing water absorption. It is expressed as a ratio of oil sorption percentage to water sorption percentage. A higher selectivity value indicates that the material is highly efficient at targeting oil, making it ideal for applications like oil spill cleanup where separating oil from water is crucial. **Figure 4** illustrates the mechanism and results of oil-to-water selectivity testing using a sample material. In Figure 4(a), the testing mechanism is shown where the sample was placed on the oil-water interface. After sorption, a high amount of oil (Os: oil sorption) was absorbed by the sample, whereas only a small amount of water (Ws: water sorption) was absorbed. This diagram visually demonstrates how the sample selectively absorbed oil from the interface while leaving the water less affected, indicating strong oil-to-water selectivity. Figure 4(c,d) provide a side view and a top view of a real selectivity test using different types of oils (food oil and engine oil) in water. It shows how the oils remain separated from the water with the sample absorbing only the oil, illustrating the material's oil sorption and resistance to water absorption.

Table 2 provides oil-to-water selectivity and oil removal efficiency for the different samples (N0 to N7). Sample N6 shows the highest food oil-to-water selectivity at 42.60, indicating a strong preference for absorbing food oil over water. Samples N1, N3, N0, N2, and N7also demonstrate notable selectivity with values of 23.02, 27.19, 29.77, 31.87, and 28.27 respectively. Sample N4 has the lowest selectivity at 16.42, followed by N5 at 14.88, suggesting these samples are less effective in distinguishing between oil and water as compared to other samples.

Sample N6 again stands out with the highest selectivity for engine oil at 40.00. Samples N1, N3, N0, N2, and N7also show good selectivity with values of 21.26, 25.31, 28.24, 29.32, and 26.49 respectively. Sample N4 and N5 have the lowest selectivity at 15.31 and 13.66 respectively, indicating poorer performance in distinguishing engine oil from water as compared to other samples. Overall, the data indicates that while all samples retain a good capacity for oil removal, the selectivity varies, with samples like N6, N7, and N2 being the most effective and reliable for repeated use in oil sorption applications.

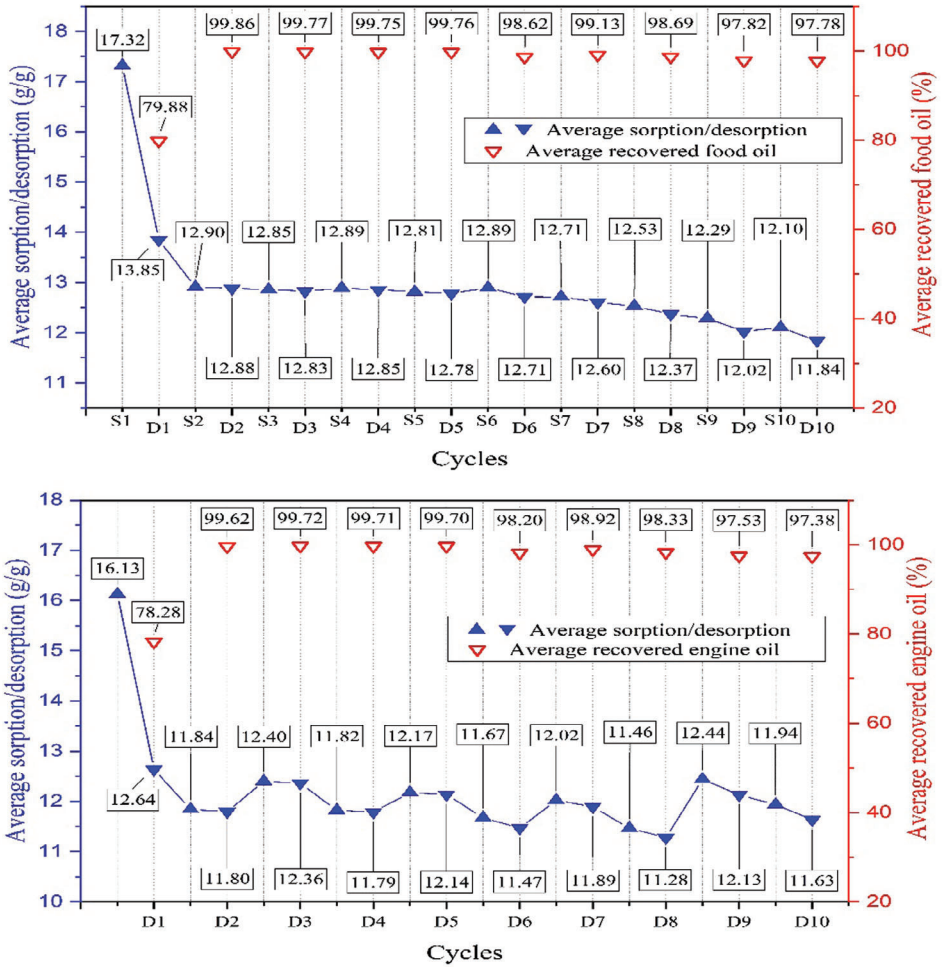

Figure 5. The reusability test result of food and engine oil sorption/desorption of samples details.

3.6. Reusability

Figure 5 and **Table 3** detail food oil sorption and desorption across multiple cycles for samples N0 to N7, including the average recovered food oil percentage. Sample N6 has the highest initial sorption at 19.45 g g^{-1}, followed by N7 at 18.78 g g^{-1} and N2 at 18.28 g g^{-1}, while N0 has the lowest at 14.58 g g^{-1}. Across cycles (S2 to S10), all samples show a decline in sorption capacity, with N0 dropping to 10.57 g g^{-1} by S10. However, the average sorption rate remains high, range 12.10 to 12.90 g g^{-1} for all samples. On the other hand, the initial average oil recovery rate (desorption) at D1 is 79.88% and remains high at 97.78 to 99.86% across cycles (D2 to D10) for all samples. N6, initially at 16.25 g g^{-1} oil desorption, retains 14.88 g g^{-1} by D10, showing moderate decline. N7 drops from 15.43 g g^{-1} desorption to 13.89 g g^{-1} by D10, indicating a less steep decline. Other samples also show steady declines but maintain high recovery rates, highlighting their reuse potential.

Figure 5 and **Table 4** detail Engine oil sorption and desorption across multiple cycles for samples N0 to N7, including the average recovered engine oil percentage. Sample N6 has the highest initial sorption at 18.26 g g^{-1}, followed by N7 at 17.59 g g^{-1} and N2 at 16.82 g g^{-1}, while N0 has the lowest at 13.83 g g^{-1}. Across cycles (S2 to S10), all samples show a decline in sorption capacity, with N0 dropping to 10.53 g g^{-1} by S10. However, the average sorption rate remains high, range 11.63 to 11.84 g g^{-1} for all samples. On the other hand, the initial average oil recovery rate (desorption) at D1 is 78.28% and remains high at 97.38 to 99.62% across cycles (D2 to D10) for all samples. N6, initially at 14.87 g g^{-1} oil desorption, retains 13.87 g g^{-1} by D10, showing moderate decline. Other samples also show steady declines but maintain high recovery rates, highlighting their reuse potential.

All samples stand out with high initial sorption and consistent recovery rates. Despite the decline in sorption capacity, the ability to recover oil remains robust, making samples suitable for repeated use in oil sorption. This analysis highlights the importance of both sorption capacity and recovery efficiency in evaluating reusable materials for oil sorption.

3.7. Statistical Analysis

Table 5 presents the results of oil sorption and retention tests conducted on various nonwoven samples (N0 to N7) using both

Table 3. The reusability test result of food oil sorption/desorption of samples details.

Cycles	Food oil sorption/desorption [g g^{-1}]								Average sorption/desorption [g g^{-1}]	Average Recovered Food oil [%]
	N0	N1	N2	N3	N4	N5	N6	N7		
S1	14.58	16.87	18.28	17.15	17.59	15.83	19.45	18.78	17.32	
D1	11.5	13.73	14.21	13.45	13.72	12.55	16.25	15.43	13.85	79.88
S2	11.43	13.74	11.42	11.88	11.73	12.28	15.89	14.86	12.90	
D2	11.40	13.71	11.40	11.87	11.72	12.26	15.87	14.85	12.88	99.86
S3	11.26	13.76	11.47	11.85	11.56	12.36	15.87	14.71	12.85	
D3	11.23	13.73	11.44	11.82	11.53	12.33	15.84	14.68	12.83	99.77
S4	10.99	13.87	11.56	11.91	11.74	12.43	15.88	14.71	12.89	
D4	10.96	13.83	11.53	11.88	11.70	12.40	15.84	14.68	12.85	99.75
S5	11.22	13.64	11.36	11.99	11.48	12.18	16.00	14.61	12.81	
D5	11.19	13.61	11.33	11.96	11.45	12.15	15.97	14.58	12.78	99.76
S6	11.58	13.89	11.60	11.88	11.58	12.20	15.76	14.62	12.89	
D6	11.40	13.72	11.42	11.71	11.41	12.02	15.59	14.44	12.71	98.62
S7	11.28	13.52	11.46	11.69	11.49	12.06	15.84	14.39	12.71	
D7	11.17	13.41	11.35	11.58	11.38	11.95	15.73	14.28	12.60	99.13
S8	10.91	13.58	11.08	11.64	11.18	11.96	15.49	14.39	12.53	
D8	10.75	13.42	10.91	11.48	11.02	11.80	15.32	14.23	12.37	98.69
S9	10.84	13.19	10.87	11.28	10.97	11.71	15.29	14.13	12.29	
D9	10.58	12.92	10.61	11.02	10.71	11.45	15.03	13.87	12.02	97.82
S10	10.57	12.94	10.68	11.15	10.70	11.58	15.09	14.10	12.10	
D10	10.28	12.66	10.39	10.86	10.41	11.36	14.88	13.89	11.84	97.78

Table 4. The reusability test result of engine oil sorption/desorption of samples details.

Cycles	Engine oil sorption/desorption [g g^{-1}]								Average sorption/desorption [g g^{-1}]	Average recovered engine oil [%]
	N0	N1	N2	N3	N4	N5	N6	N7		
S1	13.83	15.58	16.82	15.97	16.41	14.54	18.26	17.59	16.13	
D1	10.91	12.01	13.51	12.14	12.93	10.99	14.87	13.73	12.64	78.28
S2	10.45	11.82	12.48	10.10	11.45	9.88	15.41	13.15	11.84	
D2	10.41	11.59	12.47	10.08	11.43	9.86	15.40	13.13	11.80	99.62
S3	10.46	11.48	12.45	10.84	12.24	11.51	15.28	14.92	12.40	
D3	10.43	11.43	12.42	10.81	12.20	11.48	15.25	14.88	12.36	99.72
S4	9.42	12.83	11.53	10.89	11.15	9.83	15.20	13.71	11.82	
D4	9.39	12.78	11.53	10.86	11.11	9.79	15.17	13.67	11.79	99.71
S5	9.73	11.50	13.04	9.44	14.09	11.40	13.75	14.44	12.17	
D5	9.70	11.45	13.01	9.41	14.05	11.37	13.72	14.40	12.14	99.70
S6	10.18	9.11	12.76	10.31	13.65	10.49	13.65	13.21	11.67	
D6	10.00	8.85	12.58	10.14	13.42	10.29	13.46	12.99	11.47	98.20
S7	11.87	10.47	12.25	10.18	12.83	11.01	15.44	12.10	12.02	
D7	11.76	10.31	12.14	10.07	12.69	10.89	15.32	11.96	11.89	98.92
S8	10.88	9.91	12.79	10.04	12.36	9.54	13.64	12.55	11.46	
D8	10.72	9.66	12.63	9.88	12.15	9.36	13.46	12.35	11.28	98.33
S9	11.38	12.40	12.48	10.96	13.69	10.87	14.46	13.26	12.44	
D9	11.11	12.00	12.22	10.69	13.34	10.58	14.17	12.93	12.13	97.53
S10	10.53	10.35	13.04	10.68	11.63	10.82	14.11	14.33	11.94	
D10	10.24	9.91	12.76	10.40	11.25	10.58	13.87	14.06	11.63	97.38

Table 5. Statistical analysis of food and engine oil sorption and retention.

Samples	Tested Properties			
	Food oil sorption [g g^{-1}]	Engine oil sorption [g g^{-1}]	Food oil retention [%]	Engine oil retention [%]
N0	14.58	13.83	94.46	96.043
N1	16.87	15.58	92.12	93.548
N2	18.29	16.82	92.87	94.183
N3	17.15	15.97	94.38	95.696
N4	17.60	16.41	93.19	94.506
N5	15.83	14.54	91.11	92.380
N6	19.45	18.26	95.33	97.022
N7	18.78	17.59	97.93	98.828
P-value	0.00E+00	0.00E+00	9.08E-06	7.49E-08
Significance	Significant	Significant	Significant	Significant

food oil and engine oil. The p-values for all tested properties (food oil sorption, engine oil sorption, food oil retention, and engine oil retention) are extremely low (<0.05 for sorption and retention), indicating that the differences in oil sorption and retention among the samples are statistically significant. This means that the observed variations are not due to random chance, but are likely the result of differences in material composition and structure.

4. Conclusion

Oil spills have become a severe global issue, causing significant harm to public health and the environment. Nonwoven fabrics, especially those produced through needle-punching, are playing a crucial role in managing pollution and mitigating ecological damage, including from oil spills. This study evaluates the impact of multi-fiber blending and web arrangement on the oleophilic, Self-Cleaning, and oil removal efficiency of eight needle-punched nonwoven samples made from a blend of PLA, PPS, PAN, PP, and PET fibers.

The self-cleaning performance is better in samples like N3, N6, and N7, due to their higher content of hydrophobic fibers like PAN, PP, and PPS. Similarly, samples N0, N1, and N2, with equal fiber content and varying web arrangements, also demonstrated superior self-cleaning. The study also reveals that oil sorption and retention vary across samples, with those having lower surface energy and reduced polar components showing the best results. Samples with equal fiber percentages generally perform well in oil sorption, but those with cross-laid web arrangements, higher density, and low porosity (like N0) show reduced oil sorption due to tighter fiber structures. Despite the decrease in sorption capacity over time, all samples maintain high oil recovery rates, making them suitable for repeated use.

Statistical analysis confirms that the differences in both food and engine oil sorption and retention across samples are significant, driven by variations in material composition and structure. Overall, this study highlights the potential of these nonwoven materials for oil spill cleanup, emphasizing the importance of fiber type and web arrangement in achieving desired performance characteristics.

Acknowledgements

This work was supported by the National Natural Science Foundation of China (No. 51973027), and the International Cooperation Fund of Science and Technology Commission of Shanghai Municipality (No. 21130750100).

Conflict of Interest

The authors declare no conflict of interest.

Data Availability Statement

The data that support the findings of this study are available upon reasonable request.

Keywords

multi-fiber blending, needle-punched, oil-spill clean-up, oleophilic, self-cleaning

Received: September 29, 2024
Revised: December 15, 2024
Published online:

[1] Z. Zhang, H. Sun, Y. Guo, *Int. J. Eng. Sci. Technol.* **2024**, *2*, 10.
[2] E. J. Efendi, Offshore Technology Conference **2024**.
[3] V. Subramoniapillai, G. Thilagavathi, *Res. J. Text. Apparel* **2021**, *25*, 158.
[4] R. Brindha, G. Thilagavathi, S. Viju, *J. Natl. Fibers* **2020**, *17*, 1439.
[5] A. T. Hoang, X. P. Nguyen, X. Q. Duong, T. T. Huynh, *Environ. Sci. Pollut. Res.* **2021**, *28*, 28876.
[6] B. Zaarour, W. Liu, *J. Indus. Textiles* **2023**, *53*, 15280837231186652.
[7] S. Boominathan, M. Bhuvaneshwari, K. Sangeetha, K. Pachiyappan, E. Devaki, *J. Natl. Fibers* **2022**, *19*, 11193.
[8] T. Hemamalini, V. G. Dev, *J. Natl. Fibers* **2021**, *18*, 1823.
[9] J. Egan, S. Salmon, *SN Appl. Sci.* **2022**, *4*, 1.
[10] J. T. Orasugh, K. Bal, D. Chattopadhyay, S. K. Ghosh, S. S. Ray, *Ind. J. Fibre Textile Eng.* **2022**, *2*, 1.
[11] Z. Huijing, Y. Zhang, *Google Patents*, **2022**.

[12] H. M. Yesuf, H. Memon, S. R. Islam, L. Jiawei, D. Atalie, X. Zhang, X. Qin, *Textile Leather Rev.* **2024**, *7*, 235.
[13] H. M. Yesuf, S. R. Islam, D. M. Semanie, A. K. Jhatial, X. Zhang, X. Qin, *Textile Leather Rev.* **2024**, *7*, 988.
[14] X. Li, Q. Yang, K. Zhang, L. Pan, Y. Feng, Y. Jia, N. Xu, *J. Cleaner Prod.* **2022**, *375*, 134097.
[15] Z. Ahmad, M. S. Naeem, A. Jabbar, M. Irfan, Fibers for Technical Textiles. Topics in Mining, Metallurgy and Materials Engineering, (Eds: S. Ahmad, A. Rasheed, Y. Nawab), Springer International Publishing, Cham **2020**, p. 201, https://doi.org/10.1007/978-3-030-49224-3_10.
[16] G. Thilagavathi, C. Praba Karan, R. Thenmozhi, *J. Natl. Fibers* **2020**, *17*, 18.
[17] N. Haridharan, D. Sundar, L. Kurrupasamy, S. Anandan, C.-H. Liu, J. J. Wu, *Polym. Adv. Technol.* **2022**, *33*, 1353.
[18] T. Zhang, H. Tian, X. Yin, Z. Li, X. Zhang, J. Yang, L. Zhu, *J. Polym. Environ.* **2020**, *28*, 812.
[19] Z. Momenzadeh, M. Ashjari, E. Nemati Lay, M. Paki, *Adv. Compos. Mater.* 1, https://doi.org/10.1080/09243046.2024.2387413.
[20] R. Scaffaro, E. F. Gulino, M. C. Citarrella, *J. Polym. Environ.* **2023**, *31*, 3965.
[21] S. Rastogi, A. Subash, B. Kandasubramanian, *Int. J. Environ. Sci. Technol.* **2024**, *21*, 3871.
[22] X. Dong, Y. Zheng, B. Xin, L. Lin, F. Zhang, *Text. Res. J.* **2020**, *90*, 313.
[23] H. Huang, M. Liu, Y. Li, Y. Yu, X. Yin, J. Wu, S. Chen, J. Xu, L. Wang, H. Wang, *J. Mater. Sci.* **2018**, *53*, 13243.
[24] Y. Gao, Y. Qi, S. Wang, X. Zhou, L. Lyu, G. Jin, *J. Mater. Sci.* **2022**, *57*, 20531.
[25] W. Dang, J. Liu, X. Wang, K. Yan, A. Zhang, J. Yang, L. Chen, J. Liang, *Polymers* **2020**, *12*, 63.
[26] T. Adegbola, O. Agboola, O. Fayomi, *Result Eng.* **2020**, *7*, 100144.
[27] Y. Ge, Z. Fu, Y. Deng, M. Zhang, H. Zhang, *J. Mater. Sci.* **2019**, *54*, 12592.
[28] L. Maduna, South Africa: Nelson Mandela University, **2018**, 179, https://core.ac.uk/download/pdf/224301116.pdf.
[29] A. Ketema, A. Worku, *J. Chem.* **2020**, 6628404.
[30] C. Palacios-Mateo, Y. van der Meer, G. Seide, *Environ. Sci. Eur.* **2021**, *33*, 2.
[31] S. Selonen, A. Dolar, A. Jemec Kokalj, T. Skalar, L. Parramon Dolcet, R. Hurley, C. A. M. van Gestel, *Sci. Total Environ.* **2020**, *700*, 134451.
[32] M. Y. M. Zaghloul, M. M. Y. Zaghloul, M. M. Y. Zaghloul, *Compos. Struct.* **2021**, *278*, 114698.
[33] K. J. Jem, B. Tan, *Adv. Indus. Eng. Poly. Res.* **2020**, *3*, 60.
[34] H. J. Yang, Y. K. Kim, J. A. Son, I. S. Choi, S. K. Lim, *J. Appl. Polym. Sci.* **2023**, *140*, e54436.
[35] L. Zhou, K. Ke, M.-B. Yang, W. Yang, *Compos. Commun.* **2021**, *23*, 100548.
[36] Y. Yang, M. Zhang, Z. Ju, P. Y. Tam, T. Hua, M. W. Younas, H. Kamrul, H. Hu, *Text. Res. J.* **2020**, *91*, 1641.
[37] J. Eidan, I. Rasoolan, A. Rezaeian, D. Poorveis, *Construct. Build. Mater.* **2019**, *198*, 195.
[38] D. Wang, Y. Ju, H. Shen, L. Xu, *Construct. Build. Mater.* **2019**, *197*, 464.
[39] J. Wang, Q. Dai, R. Si, S. Guo, *J. Cleaner Prod.* **2019**, *234*, 1351.
[40] D.-Y. Yoo, N. Banthia, *Cement Concrete Compos.* **2019**, *104*, 103389.
[41] Y. Yu, S. Xiong, H. Huang, L. Zhao, K. Nie, S. Chen, J. Xu, X. Yin, H. Wang, L. Wang, *React. Funct. Polym.* **2020**, *150*, 104539.
[42] G. Chen, A. K. Mohanty, M. Misra, *Compos. Part B* **2021**, *209*, 108553.
[43] D. Chukov, S. Nematulloev, M. Zadorozhnyy, V. Tcherdyntsev, A. Stepashkin, D. Zherebtsov, *Polymers* **2019**, *11*, 684.
[44] A. Alassod, H. Tina, S. R. Islam, W. Huang, G. Xu, *Environ. Technol.* **2022**, *43*, 3919.
[45] T. Dong, G. Xu, F. Wang, *Ind. Crops Prod.* **2015**, *76*, 25.
[46] S. R. Islam, A. Alassod, T. Naveed, H. Dawit, K. Ahmed, J. Jiang, *J. Indust. Textiles* **2022**, *51*, 8804S.
[47] S. R. Islam, M. K. Patoary, H. D. Estifanos, I. Lugoloobi, A. H. Yousif, J. Jiang, H. Shao, *J. Indust. Textiles* **2022**, *52*, 15280837221118063.
[48] Y. Shin, K. S. Han, B. W. Arey, G. T. Bonheyo, *ACS Omega* **2020**, *5*, 13894.
[49] A. O. Ifelebuegu, A. Johnson, *Crit. Rev. Environ. Sci. Technol.* **2017**, *47*, 964.